Consistent time-step optimization in the Lattice Boltzmann method

Journal of Computational Physics, Volume 462, 1 August 2022, 111224

Tobias Horstmann[1], Hatem Touil[2], Lucien Vienne[3] Denis Ricot[4], Emmanuel Lévêque[3]

[1]German Aerospace Center (DLR)
[2]Altair
[3]Laboratoire de Mécanique des Fluides et d'Acoustique, École Centrale de Lyon - UMR 5509
[4]CS GROUP

Groupe de Travail schémas de Boltzmann sur réseau - January 10th, 2024

Context

Lattice Boltzmann method is a great tool but

- Due to the low symmetry of standard lattices, standard stream-and-collide LB algorithm reduces to an isothermal weakly compressible Navier-Stokes model:

$$\mathrm{Ma} = \frac{|\boldsymbol{u}|_{\mathsf{max}}}{c_s} \leq 0.3.$$

- LB method is by nature a compressible method.

↪ Extensive research focuses on lifting the restrictions to low Mach numbers and isothermal fluids in LB approach.

↪ Incompressible LB models only decrease the order of compressibility errors in steady flows.

Why incompressible flows matter ?

The maximum time-step is, in general, expressed as

$$\Delta t_{\mathsf{max}} = \frac{\mathrm{CFL}\ \Delta x}{v_{\max}}, \text{ where } v_{\max} = c_s + |\boldsymbol{u}|_{\mathsf{max}}$$

Courant-Friedrichs-Lewy (CFL) number: normalized maximum velocity at which flow variations can be robustly propagated by numerical scheme.

$$\Delta t_{\mathsf{max}} \approx \frac{3 \times 10^{-6}}{1 + \mathrm{Ma}} \text{ for } \mathrm{CFL} \approx 1, \Delta x \approx 10^{-3}\mathrm{m}, c_s \approx 343\mathrm{m/s}$$

Why incompressible flows matter ?

The maximum time-step is, in general, expressed as

$$\Delta t_{\mathsf{max}} = \frac{\mathrm{CFL}\ \Delta x}{v_{\max}},\ \text{where } v_{\max} = c_s + |\boldsymbol{u}|_{\mathsf{max}}$$

Courant-Friedrichs-Lewy (CFL) number: normalized maximum velocity at which flow variations can be robustly propagated by numerical scheme.

$$\Delta t_{\mathsf{max}} \approx \frac{3 \times 10^{-6}}{1 + \mathrm{Ma}} \text{ for } \mathrm{CFL} \approx 1, \Delta x \approx 10^{-3}\mathrm{m}, c_s \approx 343\mathrm{m/s}$$

For a (truly) incompressible fluid

$$\Delta t_{\max} = \frac{\mathrm{CFL}\ \Delta x}{|\boldsymbol{u}|_{\mathsf{max}}} \quad \Longrightarrow \quad \Delta t_{\max}^{incomp.} \simeq \frac{\Delta t_{\max}^{comp.}}{\mathrm{Ma}}$$

Artificial speed of sound

- In the LB method, the distribution functions move from one lattice node to another during exactly one time-step, with a characteristic speed $c = \Delta x / \Delta t$.
- On the other hand, the propagation of sound is associated to the effective transport of mass-density variations via the distribution functions.

Artificial speed of sound

- In the LB method, the distribution functions move from one lattice node to another during exactly one time-step, with a characteristic speed $c = \Delta x / \Delta t$.
- On the other hand, the propagation of sound is associated to the effective transport of mass-density variations via the distribution functions.

↪ Speed of sound and speed of microscopic propagation are physically related, for standard lattice:

$c = c_0\sqrt{3}$, where $c_0 = \sqrt{p/\rho}$ is the *isothermal* speed of sound

↪ Accelerate a LB simulation is to *artificially* decrease c_0, or equivalently, to increase the compressibility of the fluid (same as in the artificial compressibility method).

Artificial speed of sound

- × Set a targeted Ma. In unsteady simulations, maximum velocity may vary by orders of magnitude.
- ✓ Adapt Δt as a function of the current maximum flow velocity.

Artificial speed of sound

- × Set a targeted Ma. In unsteady simulations, maximum velocity may vary by orders of magnitude.
- ✓ Adapt Δt as a function of the current maximum flow velocity.
- ! It has a side effect on the distribution functions
  - N. Thürey et al. "Optimization and stabilization of LBM free surface flow simulations using adaptive parameterization", Computers and Fluids (2006)
  - J. Latt "Hydrodynamic limit of lattice Boltzmann equations". PhD thesis. Université de Genève (2007)
- ! The continuity of the pressure forces is not preserved in these algorithms.

Artificial speed of sound

- × Set a targeted Ma. In unsteady simulations, maximum velocity may vary by orders of magnitude.
- ✓ Adapt Δt as a function of the current maximum flow velocity.
- ! It has a side effect on the distribution functions
  - N. Thürey et al. "Optimization and stabilization of LBM free surface flow simulations using adaptive parameterization", Computers and Fluids (2006)
  - J. Latt "Hydrodynamic limit of lattice Boltzmann equations". PhD thesis. Université de Genève (2007)
- ! The continuity of the pressure forces is not preserved in these algorithms.

Aims of this presentation

- ⊙ Comment on this impact.
- ⊙ Propose a correction to preserve the continuity of the pressure forces.

Physical aspects of the adaptive time-stepping

The compressible Navier-Stokes equations with a fluctuated density field $\rho(\boldsymbol{x},t) = \rho_{\text{ref}} + \rho'(\boldsymbol{x},t)$ read

$$\frac{\partial \rho'}{\partial t} + \nabla\cdot(\rho\boldsymbol{u}) = 0 \qquad \& \qquad \frac{\partial \boldsymbol{u}}{\partial t} + (\boldsymbol{u}\cdot\nabla)\,\boldsymbol{u} = -\frac{1}{\rho}\nabla\left(\rho' c_0^2\right) + \nu\Delta\boldsymbol{u} + \frac{\boldsymbol{f}_{ext}}{\rho}$$

If the speed of sound is changed from c_0 to $c_0^* = \lambda c_0$

↪ By default, the above Navier-Stokes model is continuous in $\rho(\boldsymbol{x},t)$.

Physical aspects of the adaptive time-stepping

The compressible Navier-Stokes equations with a fluctuated density field $\rho(\boldsymbol{x},t) = \rho_{\text{ref}} + \rho'(\boldsymbol{x},t)$ read

$$\frac{\partial \rho'}{\partial t} + \nabla \cdot (\rho \boldsymbol{u}) = 0 \qquad \& \qquad \frac{\partial \boldsymbol{u}}{\partial t} + (\boldsymbol{u} \cdot \nabla)\, \boldsymbol{u} = -\frac{1}{\rho}\nabla\left(\rho' c_0^2\right) + \nu \Delta \boldsymbol{u} + \frac{\boldsymbol{f}_{ext}}{\rho}$$

If the speed of sound is changed from c_0 to $c_0^* = \lambda c_0$

↪ By default, the above Navier-Stokes model is continuous in $\rho(\boldsymbol{x},t)$.

- The continuity of the pressure force per unit mass requires that

$$-\frac{c_0^2}{\rho}\nabla\rho' = -\frac{(\lambda c_0)^2}{\rho^*}\nabla\rho'^* \qquad \Longrightarrow \qquad \rho^* = \rho_{\text{ref}}\left(\frac{\rho}{\rho_{\text{ref}}}\right)^{\frac{1}{\lambda^2}}.$$

This yields to a spurious source term in the mass conservation equation:

$$\frac{\partial \rho^{*\prime}}{\partial t} + \nabla \cdot (\rho^* \boldsymbol{u}) = \frac{\lambda^2 - 1}{\lambda^2}\rho^*\left(\nabla \cdot \boldsymbol{u}\right)$$

$\lambda \simeq 1$ and $\nabla \cdot \boldsymbol{u} \simeq 0$ in the weakly-compressible regime, this term remains small in practice.

Subtleties of the algorithm implementation

In the *adaptive time-stepping* algorithm, the speed of sound is tailored in order to maintain a constant target Mach number Ma_t so that

$$c_0^*(t) = \frac{u_{\max}(t)}{\mathrm{Ma}_t} = \lambda(t) c_0(t) \qquad \& \qquad \Delta t^* = \frac{1}{\lambda} \Delta t.$$

Subtleties of the algorithm implementation

In the *adaptive time-stepping* algorithm, the speed of sound is tailored in order to maintain a constant target Mach number Ma_t so that

$$c_0^*(t) = \frac{u_{\max}(t)}{\mathrm{Ma}_t} = \lambda(t) c_0(t) \qquad \& \qquad \Delta t^* = \frac{1}{\lambda}\Delta t.$$

- The stream-and-collide algorithm is usually solved in non-dimensional lattice units ($\tilde{\square}$) for which $\Delta\tilde{x} = \Delta\tilde{t} = 1$.
- Somewhat against our intuition, the speed of sound in this framework remains constant and equal to $\tilde{c}_0 = 1/\sqrt{3}$.
- The rescaled maximum fluid velocity $\tilde{u}^*_{\max}$ (in lattice units) is adapted *wrt* Ma_t.

Summary of the algorithm

1. Update g_α via streaming by using $g_\alpha(\boldsymbol{x}, t) = \widehat{g}_\alpha(\boldsymbol{x} - \boldsymbol{c}_\alpha \Delta t, t - \Delta t)$.
2. Compute ρ, $\tilde{\boldsymbol{f}}_{ext}$, $\tilde{\boldsymbol{u}}$, and g_α^{eq} to obtain g_α^{neq} by using $g_\alpha^{neq} = g_\alpha - g_\alpha^{eq} + \frac{\Delta t}{2} F_\alpha$.
3. Compute $\tilde{u}_{\mathsf{max}}$ and $\lambda = \tilde{u}_{\mathsf{max}} / \left(\tilde{c}_0 \mathrm{Ma}_t\right)$.
4. Compute ρ^* for adaptive time-stepping (ATS) with correction.
5. Compute the rescaled variables $\tilde{\boldsymbol{u}}^* = \tilde{\boldsymbol{u}}/\lambda$ and $\tilde{\boldsymbol{f}}_{ext}^* = \tilde{\boldsymbol{f}}_{ext}/\lambda^2$.
6. Compute $g_\alpha^{*\,eq}$ and $\tilde{F}_\alpha^*$ with the rescaled variables
7. Compute $\tilde{\tau}_g^*$ by using $\tilde{\tau}_g^* = \frac{1}{\lambda}\left(\tilde{\tau}_g - \frac{1}{2}\right) + \frac{1}{2}$.
8. Compute $g_\alpha^{*\,neq}$ using $g_\alpha^{*\,neq} = \frac{1}{\lambda} \frac{\rho^*}{\rho} \frac{\tilde{\tau}_g^*}{\tilde{\tau}_g}\, g_\alpha^{neq}$ together with g_α^{neq} from step 2.
9. Compute $\widehat{g}_\alpha^*$ by using $\widehat{g}_\alpha^*(\boldsymbol{x}, t) = g_\alpha^*(\boldsymbol{x}, t) - \frac{\Delta t^*}{\tau_g^*} g_\alpha^{*neq}(\boldsymbol{x}, t) + \Delta t^* F_\alpha^*(\boldsymbol{x}, t)$.

Detailed steps 5. & 7.

$$c_0^* = \lambda c_0 \qquad \& \qquad \Delta t^* = \frac{1}{\lambda}\Delta t$$

Step 5: rescaled variables $\tilde{\boldsymbol{u}}^*$, $\tilde{\boldsymbol{f}}_{ext}^*$

$$\tilde{\boldsymbol{u}}^* = \boldsymbol{u}\frac{\Delta t^*}{\Delta x} = \boldsymbol{u}\frac{\Delta t}{\Delta x}\frac{1}{\lambda} = \tilde{\boldsymbol{u}}\frac{1}{\lambda} \qquad \& \qquad \tilde{\boldsymbol{f}}_{ext}^* = \boldsymbol{f}_{ext}\frac{(\Delta t^*)^2}{\Delta x} = \frac{1}{\lambda^2}\tilde{\boldsymbol{f}}_{ext}.$$

Detailed steps 5. & 7.

$$c_0^* = \lambda c_0 \qquad \& \qquad \Delta t^* = \frac{1}{\lambda}\Delta t$$

Step 5: rescaled variables $\tilde{\boldsymbol{u}}^*$, $\tilde{\boldsymbol{f}}^*_{ext}$

$$\tilde{\boldsymbol{u}}^* = \boldsymbol{u}\frac{\Delta t^*}{\Delta x} = \boldsymbol{u}\frac{\Delta t}{\Delta x}\frac{1}{\lambda} = \tilde{\boldsymbol{u}}\frac{1}{\lambda} \qquad \& \qquad \tilde{\boldsymbol{f}}^*_{ext} = \boldsymbol{f}_{ext}\frac{(\Delta t^*)^2}{\Delta x} = \frac{1}{\lambda^2}\tilde{\boldsymbol{f}}_{ext}.$$

Step 7: rescaled relaxation time $\tilde{\tau}_g^*$

Considering that the viscosity must remain unaltered with

$$\nu = \left(\tilde{\tau}_g - \frac{1}{2}\right)\frac{c_0\Delta x}{\sqrt{3}} = \left(\tilde{\tau}_g^* - \frac{1}{2}\right)\frac{c_0^*\Delta x}{\sqrt{3}} \qquad \Longrightarrow \qquad \tilde{\tau}_g^* = \frac{1}{\lambda}\left(\tilde{\tau}_g - \frac{1}{2}\right) + \frac{1}{2}.$$

Detailed step 8. regularization as a possible option

The rescaling of g_α^{neq} is not straightforward since its projection onto moment space includes non-hydrodynamic moments, whose rescaling is not intuitive.

Regularization of g_α^{neq} (as proposed by Latt)

- Rescaling by regularization relies on the continuity of $\sum_\alpha g_\alpha^{neq} \boldsymbol{c}_\alpha \boldsymbol{c}_\alpha$.
- This expression does not lead to any particular properties at the macroscopic level.
- Regularization can induce a computational overload.

Detailed step 8.

Alternative rescaling based on the continuity of $\boldsymbol{S}$

A Chapman-Enskog analysis establishes that

$$\sum_{\alpha=0}^{q-1} g_\alpha^{neq} \boldsymbol{c}_\alpha \boldsymbol{c}_\alpha = -2\rho\tau_g c_0^2 \boldsymbol{S} + \mathcal{O}(\mathrm{Ma}^3), \quad \text{where } \boldsymbol{S} \text{ is the rate-of-strain tensor.}$$

The continuity of $\boldsymbol{S}$ then gives in lattice units

$$\frac{\sum_{\alpha=0}^{q-1} g_\alpha^{neq} \boldsymbol{e}_\alpha \boldsymbol{e}_\alpha}{\rho \tilde{\tau}_g \Delta t} = \frac{\sum_{\alpha=0}^{q-1} g_\alpha^{*\,neq} \boldsymbol{e}_\alpha \boldsymbol{e}_\alpha}{\rho^* \tilde{\tau}_g^* \Delta t^*}$$

and eventually yields

$$g_\alpha^{*\,neq} = \frac{1}{\lambda} \frac{\rho^*}{\rho} \frac{\tilde{\tau}_g^*}{\tilde{\tau}_g}\; g_\alpha^{neq}$$

by assuming that all the g_α^{neq}'s are rescaled by a same factor.

Summary of the algorithm

1. Update g_α via streaming by using $g_\alpha(\boldsymbol{x},t)=\widehat{g}_\alpha(\boldsymbol{x}-\boldsymbol{c}_\alpha\Delta t, t-\Delta t)$.
2. Compute ρ, $\tilde{\boldsymbol{f}}_{ext}$, $\tilde{\boldsymbol{u}}$, and g_α^{eq} to obtain g_α^{neq} by using $g_\alpha^{neq}=g_\alpha-g_\alpha^{eq}+\frac{\Delta t}{2}F_\alpha$.
3. Compute $\tilde{u}_{\mathsf{max}}$ and $\lambda=\tilde{u}_{\mathsf{max}}/\left(\tilde{c}_0\mathrm{Ma}_t\right)$.
4. Compute ρ^* for adaptive time-stepping (ATS) with correction.
5. Compute the rescaled variables $\tilde{\boldsymbol{u}}^*=\tilde{\boldsymbol{u}}/\lambda$ and $\tilde{\boldsymbol{f}}^*_{ext}=\tilde{\boldsymbol{f}}_{ext}/\lambda^2$.
6. Compute $g_\alpha^{*\,eq}$ and $\tilde{F}_\alpha^*$ with the rescaled variables
7. Compute $\tilde{\tau}_g^*$ by using $\tilde{\tau}_g^*=\frac{1}{\lambda}\left(\tilde{\tau}_g-\frac{1}{2}\right)+\frac{1}{2}$.
8. Compute $g_\alpha^{*\,neq}$ using $g_\alpha^{*\,neq}=\frac{1}{\lambda}\frac{\rho^*}{\rho}\frac{\tilde{\tau}_g^*}{\tilde{\tau}_g}\,g_\alpha^{neq}$ together with g_α^{neq} from step 2.
9. Compute $\widehat{g}_\alpha^*$ by using $\widehat{g}_\alpha^*(\boldsymbol{x},t)=g_\alpha^*(\boldsymbol{x},t)-\frac{\Delta t^*}{\tau_g^*}g_\alpha^{*neq}(\boldsymbol{x},t)+\Delta t^*F_\alpha^*(\boldsymbol{x},t)$.

Natural convection in thermal flow

Temperature-driven buoyancy force (Boussinesq hyptothesis):

$$\boldsymbol{f}_b(\boldsymbol{x},t) = \rho(\boldsymbol{x},t)\boldsymbol{g}\beta\left(T(\boldsymbol{x},t) - T_0\right)$$

where β is the coefficient of thermal expansion of the fluid, $\boldsymbol{g}$ is the gravitational acceleration and T_0 is the temperature at rest.

Initial hot spot (plume): $T(\boldsymbol{x},t_0) = T_0 + exp\left(-\frac{x^2+y^2}{R^2}\right)\Delta T$

Hybrid finite-difference scheme / LB scheme

$$\frac{\partial T}{\partial t} + (\boldsymbol{u}\cdot\nabla)T = \kappa\nabla^2 T \quad \Longrightarrow \quad T(\boldsymbol{x},t+1) = T(\boldsymbol{x},t) - (\tilde{\boldsymbol{u}}\cdot\nabla_h)T + \tilde{\kappa}\Delta_h T$$

where ∇_h and Δ_h stand for finite-difference gradient and Laplacian operators.

$\tilde{\kappa}^* = \nu\Delta t^*/Pr\Delta x^2$ with the Prandtl number $Pr = \nu/\kappa$.

Diagram of the Adaptive Time-Stepping (ATS) algorithm

To avoid abrupt changes at the beginning of the simulation:

$$c_0^* = \max\left(\frac{u_{\text{max}}}{\text{Ma}_t}, c_0^{0.9}\right)$$

where $\text{Ma}_t = 0.15$.
Δt is reevaluated every 10 iterations.

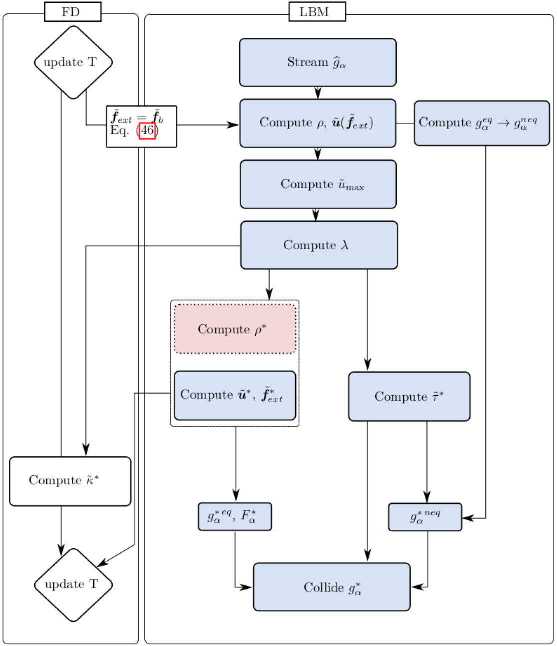

2D field: temperature [K] ($\Delta T = 10$) at 45.2 s

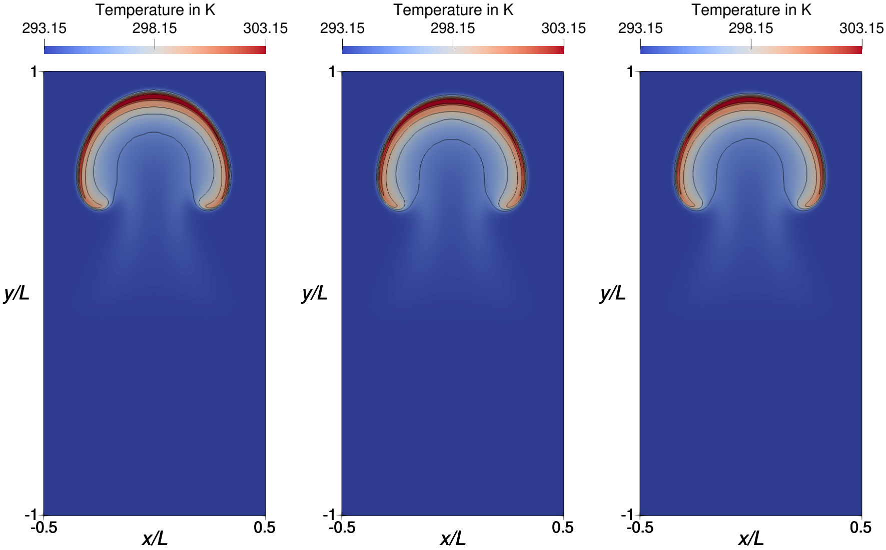

(a) constant time-step at iteration 67310 (b) ATS at iteration 3690 (c) ATS with correction at iteration 3690

2D field: velocity norm $[\mathrm{ms}^{-1}]$ $(\Delta T = 10)$ at 45.2 s

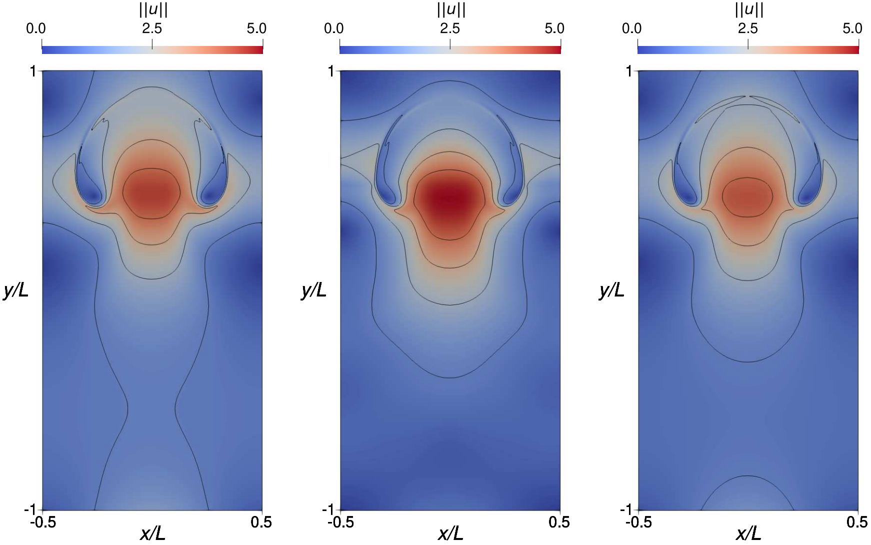

(a) constant time-step at iteration 67310 (b) ATS at iteration 3690 (c) ATS with correction at iteration 3690

Rise of the thermal plume over a duration (physical time) of 45.3 s.

(───): constant time-step
(·····): ATS
(───): ATS with correction
! Iterations in log-scale

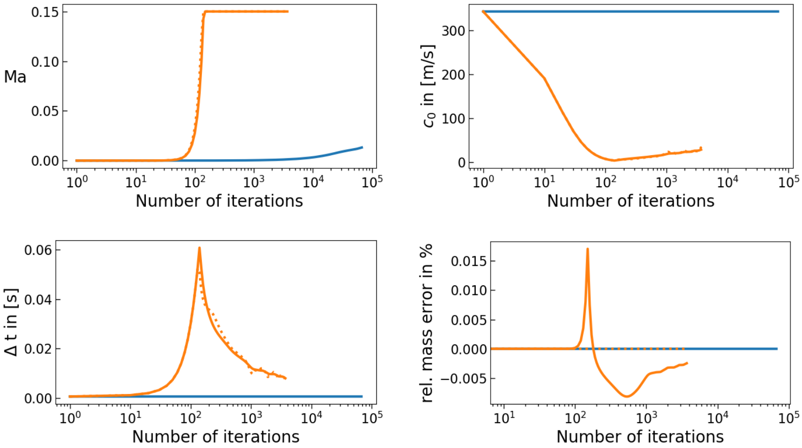

- Qualitative agreement
- $\sim 20\times$ benefit for ATS
- ATS: oscillations at the end of the run (Δt plot)
- ATS with correction: mass error $[-0.008\%, 0.017\%]$

Womersley flow: a pulsating 2D channel flow

The pressure gradient oscillates according to

$$\frac{\partial P}{\partial x} = A\cos(\omega t)$$

The problem has an exact solution in the laminar regime

$$u_x(y,t) = \Re\left\{\imath\,\frac{A}{\rho\,\omega}\left(1 - \frac{\cos(\Lambda\,(\frac{2y}{L_y} - 1))}{\cos(\Lambda)}\right)e^{\imath\,\omega\,t}\right\}$$

$$u_y = 0$$

with $\Lambda^2 = -\imath\,\alpha^2$ and $\alpha^2 = \frac{L_y^2\,\omega}{4\,\nu}$.

Here $\alpha = 2.59$, $Re = 100$ and $\tilde{T} = 5000$ to mimic real life flow phenomena that can be encountered in the smaller arteries of the human body.

Womersley flow: a pulsating 2D channel flow

The pressure gradient oscillates according to

$$\frac{\partial P}{\partial x} = A\cos(\omega t)$$

The problem has an exact solution in the laminar regime

$$u_x(y,t) = \Re\left\{\imath\,\frac{A}{\rho\,\omega}\left(1 - \frac{\cos(\Lambda\,(\frac{2y}{L_y} - 1))}{\cos(\Lambda)}\right)\,e^{\imath\,\omega\,t}\right\}$$

$$u_y = 0$$

with $\Lambda^2 = -\imath\,\alpha^2$ and $\alpha^2 = \frac{L_y^2\,\omega}{4\,\nu}$.

Here $\alpha = 2.59$, $Re = 100$ and $\tilde{T} = 5000$
to mimic real life flow phenomena that can be encountered in the smaller arteries of the human body.

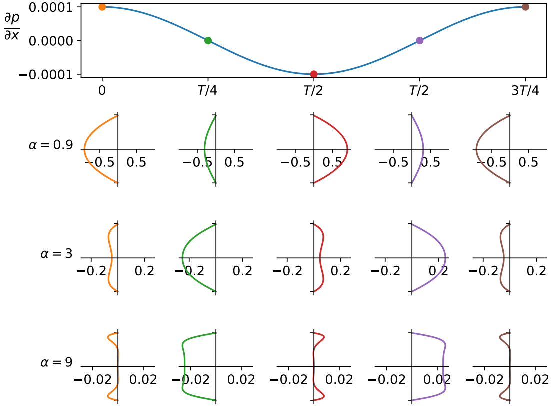

Temporal evolution of the pressure gradient (top) and the corresponding velocity profile $u_x(y,t)/U_0$ for different values of the Womersley number α.

Womersley flow: body force vs inlet/outlet boundary conditions

The pressure gradient can either be established by two strategies:

1. an external body force to every nodes of the fluid

$$\boldsymbol{f_{ext}}(t) = -A\cos(\omega t)\boldsymbol{e}_x$$

2. the inlet/outlet density boundary conditions

$$\rho_{\mathrm{in}}(t) = \rho_{\mathrm{ref}} - \frac{AL_x}{2c_0^2(t)}\cos(\omega t) \quad \text{and} \quad \rho_{\mathrm{out}}(t) = \rho_{\mathrm{ref}} + \frac{AL_x}{2c_0^2(t)}\cos(\omega t).$$

This induces the pressure gradient through the momentum equation. It is expected that the continuity of the pressure forces will have an impact.

Womersley flow: probe at the center of the oscillating channel

(▬▬): constant time-step
(▪▪▪▪▪): ATS
(▬▬): ATS with correction
$\mathrm{Ma}_t = 0.15$
ATS is activated at
$\tilde{t} = t/T = 0.75$.

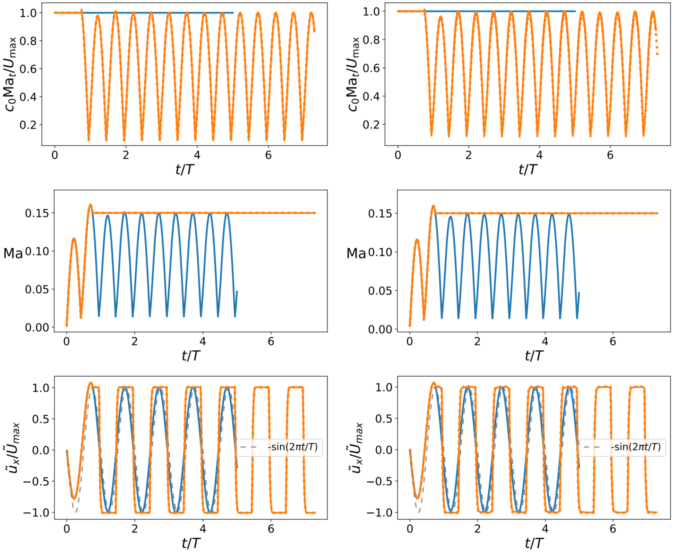

- No difference between forcing strategies or correction in ATS
- Maximum theoretical gain: $\pi/2 \approx 1.57$
- ATS speedup $\times 1.53$

Left: body-force stirring **Right:** inlet/outlet conditions

Womersley flow: velocity profile at the center of the oscillating channel

(▬▬): constant time-step
(·····): ATS
(▬▬): ATS with correction

$$\varepsilon_u(t) = \frac{\|u - \bar{u}\|_{L_2}}{\|\bar{u}\|_{L_2}} = \sqrt{\sum_y \left(u_x(\frac{L_x}{2}, y, t) - \bar{u}_x(y,t)\right)^2 \Big/ \sum_y \bar{u}_x(y,t)^2}$$

where $\bar{u}_x$ is the analytical solution.

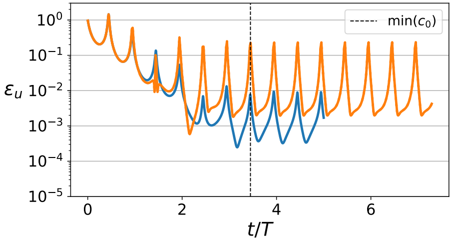

Left: body-force stirring

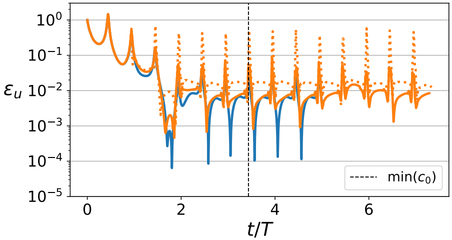

Right: inlet/outlet conditions

- Error peak when $\bar{u}_x \to 0$, $\varepsilon_u \to \infty$ (flow reversal).
- Body-force ATS errors: one order of magnitude higher *wrt* constant Δt.
- Inlet/outlet ATS with correction error: same order of magnitude *wrt* constant Δt.

Womersley flow: convergence rate of the ATS algorithms

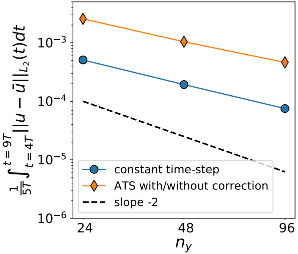

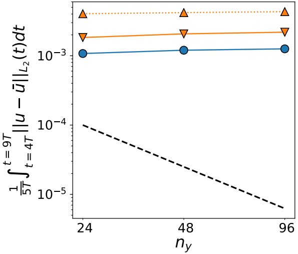

At $\mathrm{Ma}_t = 0.15$

- Body-force ATS no influence of the correction
- Inlet/outlet ATS error independent of the resolution

$\hookrightarrow$ Phase shift due to compressibility effects *wrt* incompressible solution

Left: body-force stirring

Right: inlet/outlet conditions

Womersley flow: convergence rate of the ATS algorithms

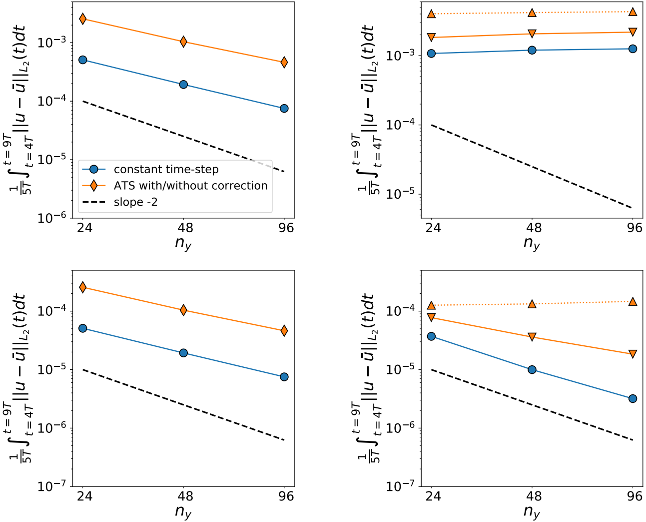

Left: body-force stirring **Right:** inlet/outlet conditions

At $\mathrm{Ma}_t = 0.15$

- Body-force ATS no influence of the correction
- Inlet/outlet ATS error independent of the resolution

$\hookrightarrow$ Phase shift due to compressibility effects *wrt* incompressible solution

At $\mathrm{Ma}_t = 0.015$

- Inlet/outlet ATS 2^{nd}-order convergence
- Inlet/outlet ATS with correction improves the accuracy

Channel entrance flow

- Increase the previous channel length by $\times 20$
- Dirichlet pressure boundary condition at the outlet
- Dirichlet velocity boundary condition at the inlet
- Initial fluid at rest and initial ramp for the velocity at the inlet:

$$U_{\text{in}}(t) = \sin\left(\frac{\pi}{2}\frac{t}{T_{\text{ramp}}}\right) U_{\text{bulk}} \qquad \text{for} \quad t \leq T_{\text{ramp}}$$

$$U_{\text{in}}(t) = U_{\text{bulk}} \qquad \text{for} \quad t > T_{\text{ramp}}$$

with $U_{\text{bulk}} = 0.75 U_0$ and $\tilde{T}_{\text{ramp}} = 10000 = \frac{1}{5}\tilde{T}_{\text{tot}}$.

- ATS is activated when Ma > 0.03

Probe at $x = 0.8 L_x$,
where the flow reaches a Poiseuille parabolic velocity profile ($U_{max} = U_0$) when $t \gg T_{\text{ramp}}$

Channel entrance flow: time evolution

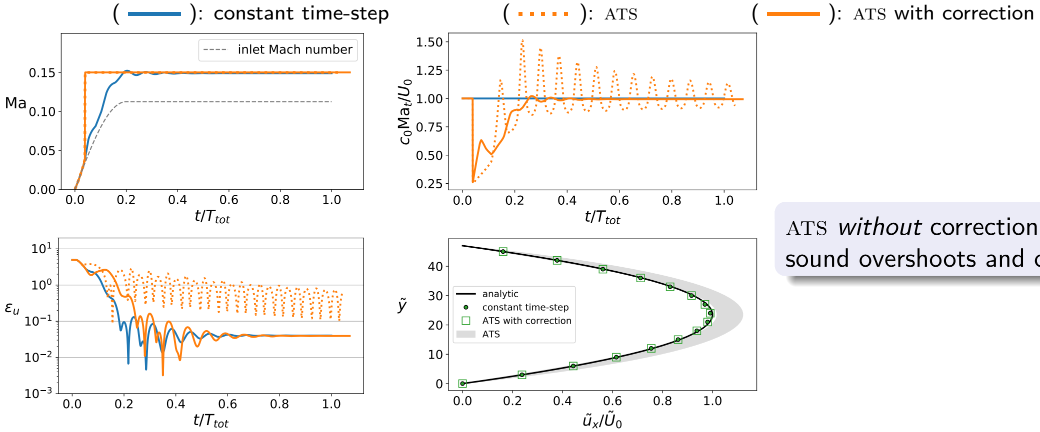

ATS *without* correction: speed of sound overshoots and oscillates

There is no free-lunch

- ATS does not always improve the (initial) convergence.
- When $c_0 \searrow$, pressure waves take longer to dissipate.

Conclusion

Adaptative time-stepping (ATS) in LB method

ATS introduces an error in either mass or momentum conservation:

- preserving the continuity of the density field instead of the pressure force (per unit mass)
- preserving the continuity of the pressure force (per unit mass) instead of the density field

Advantages of the ATS

- No prior knowledge about the maximum velocity is required
- Speed up can be considerable by optimally adapting on the flow dynamics:
  e.g. biological flows, transient thermal flows and oscillating flows in general, where the maximum velocity undergoes large variations.

We show that

ATS does not always improve the (initial) convergence.

ATS with *pressure correction* performs better:

- natural convection
- channel flows with inlet/outlet boundary conditions

Conclusion

Defining the relative change of the time-step $\varepsilon = \frac{\Delta t^* - \Delta t}{\Delta t}$

- Continuity of the density field ($\rho^* = \rho$) yields a relative error on the pressure force

$$\left(\frac{p^* - p}{p}\right) \sim \left(\frac{{c_0^*}^2 - c_0^2}{c_0^2}\right) \sim \varepsilon.$$

- Continuity of the pressure force (per unit mass) yields a relative error on the density field

$$\left(\frac{\rho^* - \rho}{\rho}\right) \sim \varepsilon \, \frac{\rho - \rho_{\text{ref}}}{\rho} \sim \varepsilon \, \text{Ma}^2,$$

↪ This provides a plausible justification for the advantage of considering the continuity of the pressure force (per unit mass) in the ATS.

Thank you for your attention

Cryospray ANR - open Ph.D. position

LATTICE BOLTZMANN SIMULATIONS OF THE DESTABILIZATION AND FRAGMENTATION OF A LIQUID INTO DROPLETS BY A FAST GAS STREAM

Numerical simulation of a kerosene flow destabilized by a crossflow of air

E. Lévêque and J.-P. Matas, Laboratory of Fluid Mechanics and Acoustics, École Centrale de Lyon